

## Effect of tube shape on the performance of a fin and tube heat exchanger

D. Sahel<sup>1</sup>, H. Ameer<sup>2,\*</sup> and M. Mellal<sup>3</sup>

<sup>1</sup>Department of Technical Sciences, University Amar Telidji-Laghouat, Algeria

<sup>2</sup>Department of Technology, University Centre of Naama, Po. Box 66, 45000, Algeria

Phone: +213770343722

<sup>3</sup>Faculty of Mechanical Engineering, USTO-MB, Oran, Algeria.

**ABSTRACT** – A numerical study is carried out to test the effect of tube shape on heat transfer and fluid flow in a finned tube heat exchanger. The effects of different shapes (circular, flat, elliptical and oval in both orientations: left and right) are analyzed. The simulations are carried out for two-dimensional and external flow of an incompressible fluid with Reynolds numbers varying between 3000 and 20000. The results obtained indicate that the shape of the tube directly affects the thermal and dynamic behaviors of a fin and tube heat exchanger. Where the circular tube ensures higher heat transfer coefficient of about 18% than the flat tube, and it generate a moderate pressure drop of about 10% in the same conditions. Also, some reliable empirical correlations are proposed to predict the Nusselt number and the friction factor.

### ARTICLE HISTORY

Revised: 4<sup>th</sup> Jan 2020

Accepted: 22<sup>nd</sup> Jan 2020

### KEYWORDS

*Heat transfer;*  
*fin and tube heat exchanger;*  
*shape of the tube;*  
*turbulent flow.*

## INTRODUCTION

Tubular bundles are essential equipment for designing fin and tube heat exchangers, where the tube design plays a vital role in improving the heat transfer phenomenon in these systems. Usually, the circular tube is widely used in the design of fin and tube heat exchangers [1-7]. The thermal performance of heat exchangers is very low by using gaseous fluids compared to liquid fluids. In contrast, the convection resistance of the gaseous fluid is generally dominant due to the thermophysical properties of the gaseous fluid [8, 9]. Besides, the tube orientation has considerable effects on the thermal performance of such systems [10].

In a thorough search, Tahseen et al. [11] reported that the flat tubes are vital equipment in various industrial applications such as modern heat exchangers, automotive radiators, air conditioning, and other applications. Compared with circular tube heat exchangers, they found that the flat tube heat exchangers have a lower friction factor and considerable heat transfer rates. In the same context, Benarji et al. [12] confirmed that the sound and vibration are low for a flat tube relative to the circular tube. They also proposed correlations to predict the Nusselt number and friction factor, taking into account the effect of the longitudinal and transverse tube ratios on heat transfer and pressure drop. Although the flat tube is recommended in the design of heat exchangers, there are several works in the literature on this research axis that have confirmed that the tube shape remains a necessary geometric parameter to be optimized [13-17]. Yogesh et al. [18] numerically investigated the fluid flow and heat transfer characteristics of a fin and tube heat exchanger having elliptical tubes of various elliptical ratios and different angles of elliptical tube orientation. They reported that the friction factor varies proportionally with the tube inclination and elliptical rate, whereas it decreases with the rise of Reynolds number. Recently, Li et al. [19, 20] confirmed that the flat tube merits to be considered in the design of fin and tube heat exchangers. In addition of the importance of the fin shapes on the thermal performances of fin and tube heat exchangers [21], Sahel et al. [22] reported in its numerical study that in the presence of vortex generators inside tubes bank; the flat tubes create better heat transfer execution compared with circular cells. Han et al. [23] numerically investigated the fluid flow and heat transfer behaviors of finned tube heat exchangers. They examined the effects of different oval and circular tubes. They concluded that using the oval fin-tube can not only decrease the flow resistance but also enhance the heat transfer performance of the heat exchangers. Also, As compared with the big circle-tube louver fin, the heat transfer coefficient of finned oval tube is augmented by 1.5–4.9%, while the pressure loss is reduced by 22.0–31.8%. Lavasani et al. [24] experimentally verified the thermal execution of a cam-shaped tube bank. They showed that the pressure loss and heat transfer rate of cam shaped tubes depend on the position of tubes in the tube bank. Also, the thermal performance factor of the cam shape tube is about six times better than that for the circular tube. Tahseen et al. [25] studied the thermal and hydrodynamic performances of airflow in an in-line flat tube bundle, and they showed that the arrangement of tubes presents another parameter, which is need to analyzing. In the same field, Zhang et al. [26] reported that wake region formed in the downstream of the flat tube may be rectified in using vortex generators.

In this article and given the importance of tube shape on heat transfer and fluid flow, a numerical investigation is carried out on the influence of different forms of the tube (circular, flat, elliptical and oval) on the thermal and dynamic behaviors of a finned tube heat exchanger. Effects of the fins are not explored in this study, and we based in our investigation only on the shape of tubes. The obtained results show that the circular-shaped tube ensures the best heat

transfer coefficient, compared to the other cases. However, the elliptical tube yields the lowest pressure losses compared to the other configurations. Then, reliable correlations have been proposed to predict the Nusselt number and the friction factor.

## GEOMETRY OF THE PROBLEM STUDIED

The geometry of the problem under investigation is illustrated in Figure 1. It concerns a finned tube heat exchanger, where different shapes of the tube are realized. The in-line arrangement of tubes was analyzed in this study. Three rows of tubes and four tubes in each row were also studied. The extended regions in the inlet and outlet of the section are essential for flow developing in these sections. Nevertheless for identical comparison with available data we used the real configurations which exist in literature. The geometrical configuration of the tube allows the use of the symmetry option to reduce the calculation time. The outer diameter of the tube ( $D$ ) is 10.55 mm, the transverse tube advance ( $P_t$ ) is 25.4 mm, and the longitudinal tube advance ( $P_l$ ) is 22 mm. Where the length of flat, elliptical, oval RO, and oval LO tubes equal to  $2D$ . The Aluminum was used as a construction material of tubes and fins, where its thickness is neglected since the present work out to analyzing only the convective heat transfer of different shaped tubes.

The profiles of velocity and temperature of airflow are recognized in the inlet section. The thermo-physical properties of air are summarized in Table 1. A uniform velocity  $U = U_{in}$  and a constant temperature  $T_{in} = 300$  K are utilized in the entry of the section. At the outlet, and for all variables, the conditions of Neumann boundary are utilized, thus the gradients of streamwise variables are set to be zero. Symmetry boundary conditions are exploited for the upper and lower sides. No-slip wall and impermeable boundary conditions have been employed over the tube wall. The constant temperature at the tube walls ( $T_w$ ) is set at 350 K.

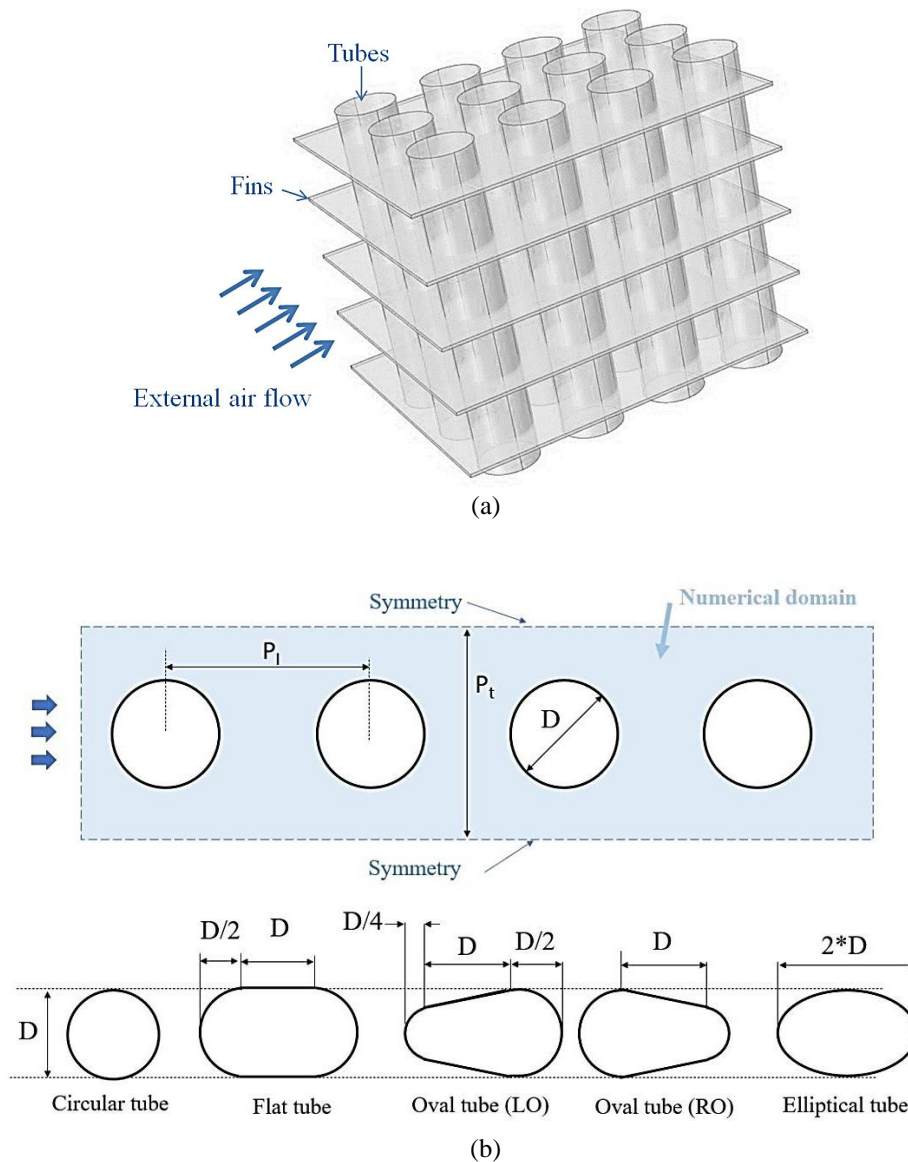


**Figure 1.** Geometry of: (a) FTHE and the (b) different tube shapes under investigation.

**Table 1.** Thermo-physical properties of air.

Density [kg/m <sup>3</sup> ]	Cp [J/kg K]	Thermal conductivity [W/m K]	Viscosity [kg/m s]
1.225	1006.43	0.0242	1.7894 x 10 <sup>-5</sup>

## MATHEMATICAL EQUATIONS AND GOVERNED PARAMETERS

The numerical model for fluid flow and heat transfer in a fin and tube heat exchanger is based on the average equations of Navier-stocks, and the energy equation.

Continuity equation:

$$\frac{\partial}{\partial x_i}(\rho u_i) = 0 \quad (1)$$

Momentum equation:

$$\frac{\partial}{\partial x_i}(\rho u_i u_j) = \frac{\partial}{\partial x_i} \left[ \mu \left( \frac{\partial u_i}{\partial x_j} - \overline{\rho u'_i \rho u'_j} \right) \right] - \frac{\partial p}{\partial x_i} \quad (2)$$

Energy equation:

$$\frac{\partial}{\partial x_i}(\rho u_i T) = \frac{\partial}{\partial x_i} \left( (\Gamma + \Gamma_t) \frac{\partial T}{\partial x_j} \right) \quad (3)$$

where  $\Gamma$  is the molecular thermal diffusivity,  $\Gamma_t$  is the turbulent thermal diffusivity:

$$\Gamma = \mu / Pr ; \Gamma_t = \mu_t / Pr_t ; \mu_t = \rho C_\mu (k^2 / \varepsilon) \quad (4)$$

The standard model of turbulence  $k$ - $\varepsilon$  which is based on the turbulent kinetic energy  $k$  (Eq. (5)) and the dissipation energy  $\varepsilon$  (Eq. (6)) is used in this study.

$$\frac{\partial}{\partial x_j}(\rho k u_i) = \frac{\partial}{\partial x_j} \left[ \left( \mu + \frac{\mu_t}{\sigma_k} \right) \frac{\partial k}{\partial x_j} \right] + G_k + \rho \varepsilon \quad (5)$$

$$\frac{\partial}{\partial x_i}(\rho \varepsilon u_i) = \frac{\partial}{\partial x_j} \left[ \left( \mu + \frac{\mu_t}{\sigma_\varepsilon} \right) \frac{\partial \varepsilon}{\partial x_j} \right] + C_{1\varepsilon} \frac{\varepsilon}{k} - C_{2\varepsilon} \rho \frac{\varepsilon^2}{k} \quad (6)$$

In these equations,  $G_k$  represents the turbulent kinetic energy generated by the average velocity gradients. The empirical constants for the  $k$ - $\varepsilon$  standard model are assigned the following values:

$$C_\mu = 0.09; C_{1\varepsilon} = 1.44; C_{2\varepsilon} = 1.92; \sigma_k = 1.0; \sigma_\varepsilon = 1.3$$

This model is widely used in the literature, (see for example [27-29]). In addition, Eiamsa-ard et al. [30] tested several turbulence models and reported that the RNG and the standard  $k$ - $\varepsilon$  turbulence models generally provide better agreement with available experiments data than others. Where, they selected the  $k$ - $\varepsilon$  model to use in prediction of complex flow. For all these reasons, we used the standard  $k$ - $\varepsilon$  model in our work.

Total heat transfer rate:

$$Q = m_f C_p (T_{out} - T_{in}) \quad (7)$$

The logarithmic mean temperature difference:

$$\Delta T_{lm} = \frac{((T_{wall} - T_{in}) - (T_{wall} - T_{out}))}{\ln((T_{wall} - T_{in}) / (T_{wall} - T_{out}))} \quad (8)$$

The heat transfer coefficient given as:

$$h = Q / (A \Delta T_{lm}) \quad (9)$$

Nusselt number: the heat transfer coefficient is represented by the Nusselt number which is given by:

$$Nu = \frac{h D_h}{K_f} \quad (10)$$

where,  $K_f$  is the thermal conductivity of fluid (air). The Reynolds number is defined as:

$$Re = \frac{u D_h}{\mu} \quad (11)$$

The friction factor ( $f$ ) is calculated along the section as:

$$f = \frac{2}{(L/D_h)} \frac{\Delta P}{\rho U_{in}^2} \quad (12)$$

## NUMERICAL MODEL

The choice and the sensitivity of the mesh play a primordial role in any numerical investigation. A series of mesh tests were performed for all computational domains presented in this work. A non-uniform triangular mesh (Figure 2) was refined near the tubes to detect the temperature and velocity gradient.

The series of mesh chosen in the case of circular tubes with  $Re = 3000$  are 64253, 91891, 111980, 145896, and 181442. From 111980 nodes, the variation of Nusselt number is not significant (does not exceed 3%) with an increased density of mesh. Table 2 illustrates the grid test for the circular tube. Therefore, our work will be based on the mesh of 111980 nodes for the following calculations. We note that the same strategy has been applied to other configurations.

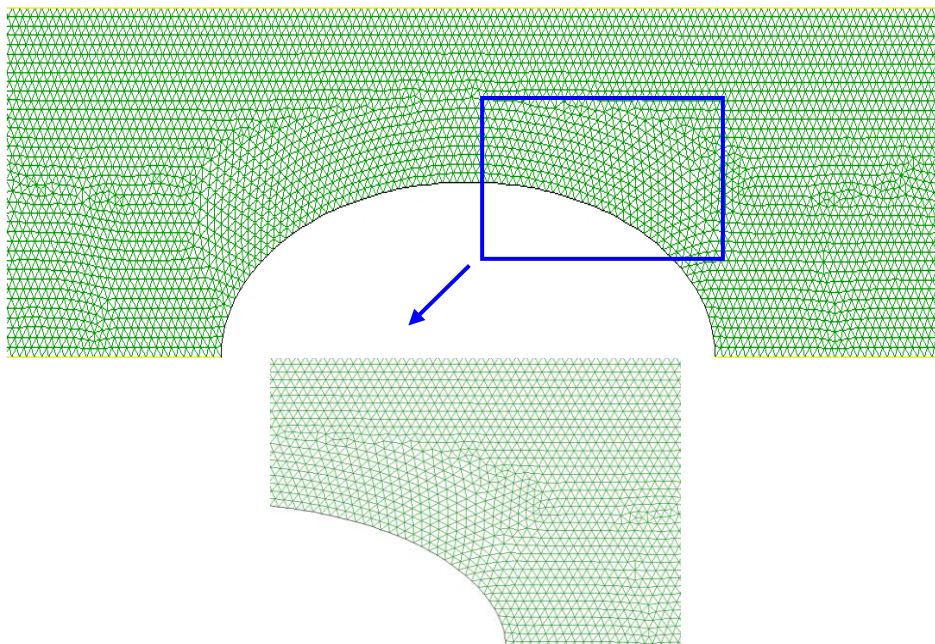


**Figure 2.** Example of generated non-uniform triangular mesh.

The commercial software ANSYS Fluent 15.0 was utilized to carry out the simulation. The governing equations with agreeing boundary conditions were solved by using the finite volume method, based on the SIMPLE algorithm (*Semi-Implicit Method for Pressure- Linked Equations*) for the velocity-pressure coupling. SIMPLE algorithm facilitates the

run convergence and also largely used in the literature [31-37]. We note that the steady-state condition has been considered for all simulations. The convective terms in governing equations for momentum and energy are discretized with the second upwind scheme.

For the convergence, default under-relaxation factors were used. The convergence criteria for the normalized residuals were fixed at  $10^{-5}$  for the flow equations and  $10^{-9}$  for the energy equation.

**Table 2.** Mesh sensibility.

Grids	Nusselt number	Error (%)
64253	68.8	-
91891	60.8	-
111980	47.9	(selected grid)
145896	49.1	2.44
181442	48.8	1.84

## RESULTS AND DISCUSSIONS

### Validation of the numerical model

Zukauskas [2] analyzed by experiments several cases with air and water, where the current investigation presents only one case among those studied by Zukauskas. Hence, the comparison was made with the same available conditions in [2].

Figure 3 presents a comparison of the Nusselt number results of the present work and that calculated by the Zukauskas [2] and Kim [38] correlations. The good agreement observed in this figure allowed the validation of our numerical model. Where the maximum deviation is observed for  $Re = 20000$ . The comparison with the present results reported that there is a difference of 9% and 5% for Kim and Zukauskas correlations, respectively. Zukauskas correlation presents a reference in the field of fin and tube heat exchangers. Where the conditions of the present study are very adopted with Zukauskas experiment. Where the Kim correlation is developed on the basis of Zukauskas correlation by adding of longitudinal pitch ratio.

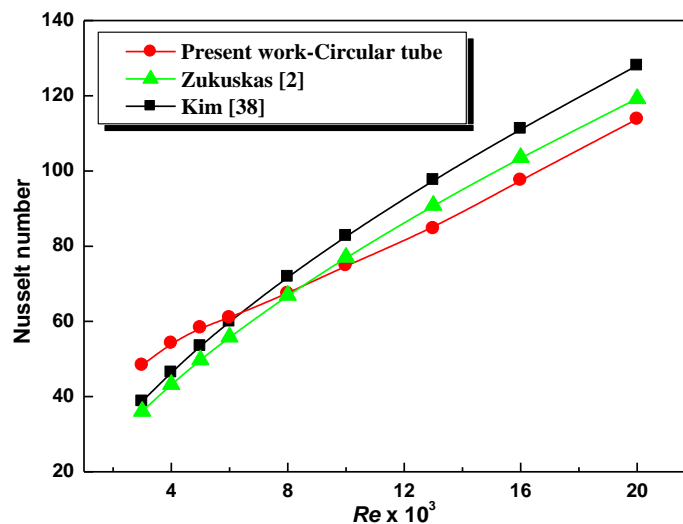


**Figure 3.** Validation of results.

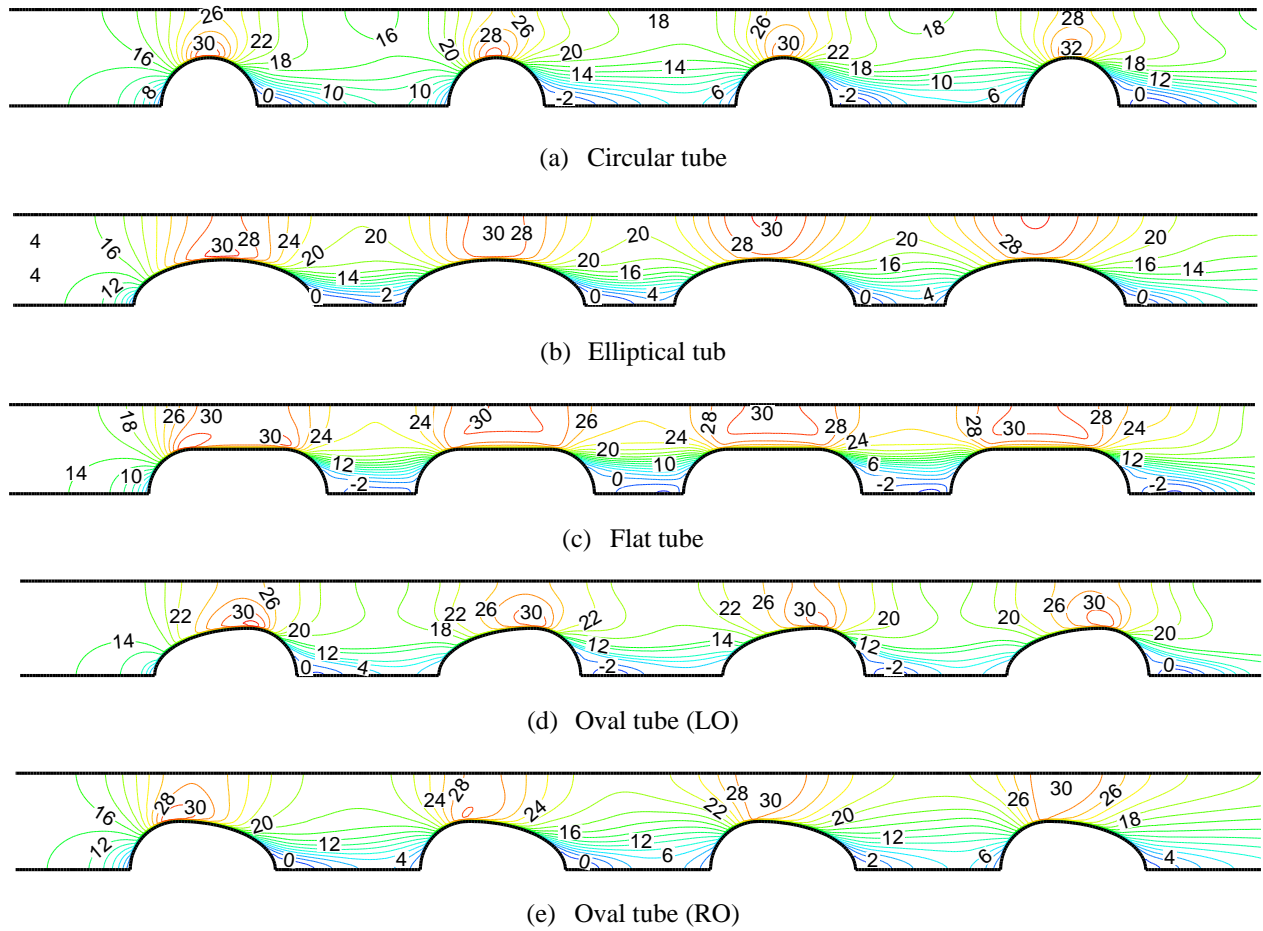
### Hydro Dynamic and Thermal Aspects

Figure 4(a-e) shows the axial velocity distribution for the different shapes studied in this work. As shown on this figure, the main flow passes around the tube while a secondary recirculation zone appears behind the tube. The flow velocity in the secondary zones is lower than that of the main jet. Unfortunately, the formation of secondary recirculation zones behind the tubes is an undesirable phenomenon for the execution of the heat transfer phenomenon.

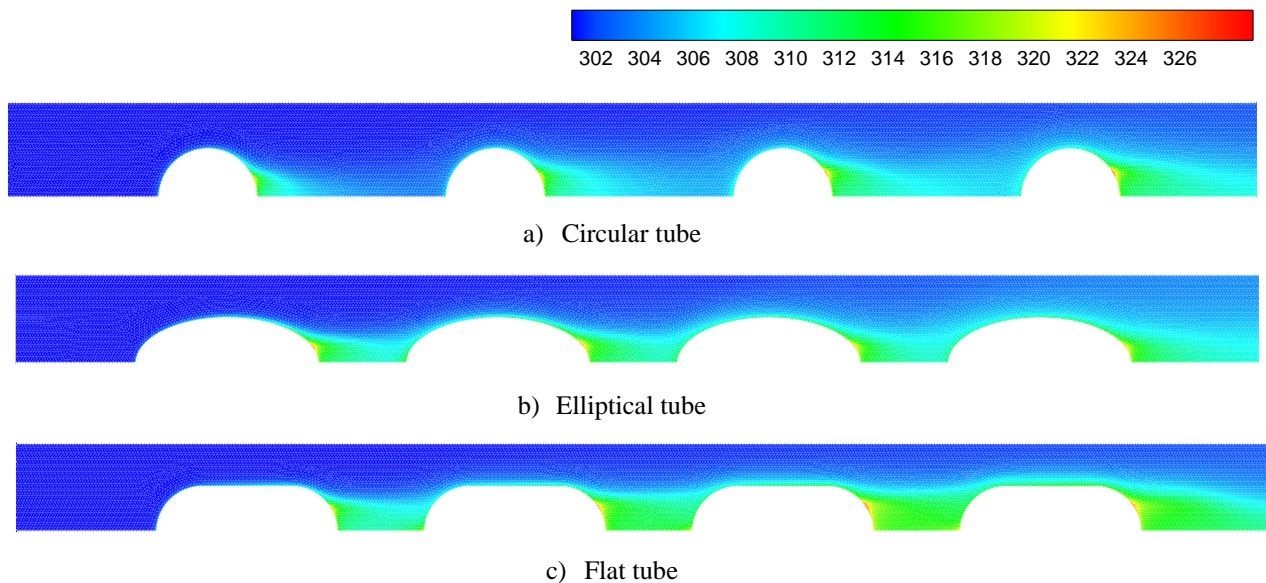
As such, the enlargement or the change of the tube shape is an additional problem on the thermal performance of the fin and tube heat exchangers, where the flat surface of the tube allows developing the hydrodynamic boundary layer.

Therefore, the thermal boundary layer may also appear on the flat surface of the tube. Then, the formation of secondary recirculation zones, the thermal and hydrodynamic boundary layers are the leading causes that can reduce the heat transfer coefficient.

There is a significant association between the formation of low-velocity areas (dead zones) and the formation of hot points behind the tubes. Figure 5 displays this association, while the fluid-structure effects directly on the thermal behaviors of FTHEs. Indeed, the rise in velocity fluctuations helps to decrease the formation of lower heat transfer areas, and consequently, it enhances FTHE performance.



**Figure 4.** Distribution of the axial velocity (unit in m/s).



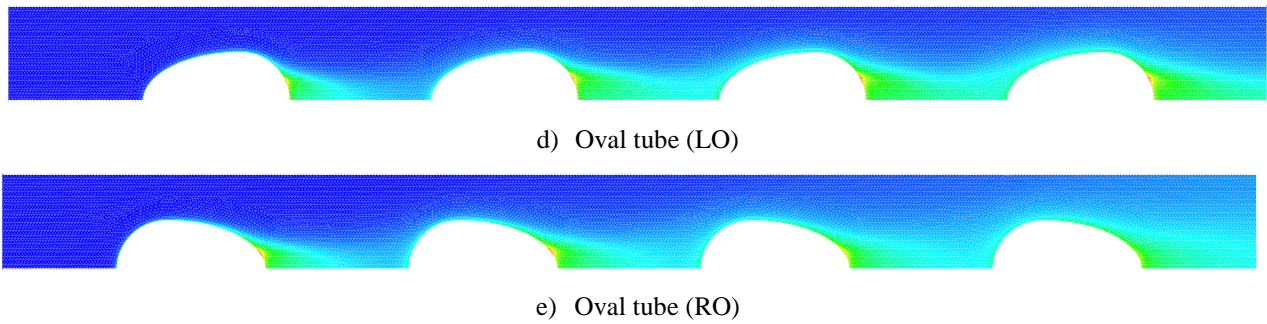


Figure 5. Temperature contours [unit in K].

**Nusselt Number**

Figure 6 shows the distribution of Nusselt number vs. Reynolds number. The highest values of Nusselt numbers are obtained with the circular tube, followed by the oval tube in the right orientation (RO), oval tube in the left orientation (LO), elliptical tube, and then the flat tube. This latter represents the low rate of heat transfer due to the training thermal boundary layer on the flat surface [23]. Comparing with the flat tube, circular, oval RO, oval LO, and elliptical tubes provide a percentage of heat transfer coefficient of about 18, 12, 10, and 4%, respectively. The superiority of the circular tube compared with the other cases is due to the highest surface of contact between airflow and the tube. Also, the hot points are very small behind the tube. With the help of Excel Software and to predict the heat transfer coefficient, Table 3 summarizes the empirical correlations of each configuration. Where  $R^2$  ( $R$ -square) is the coefficient of determination of correlation.

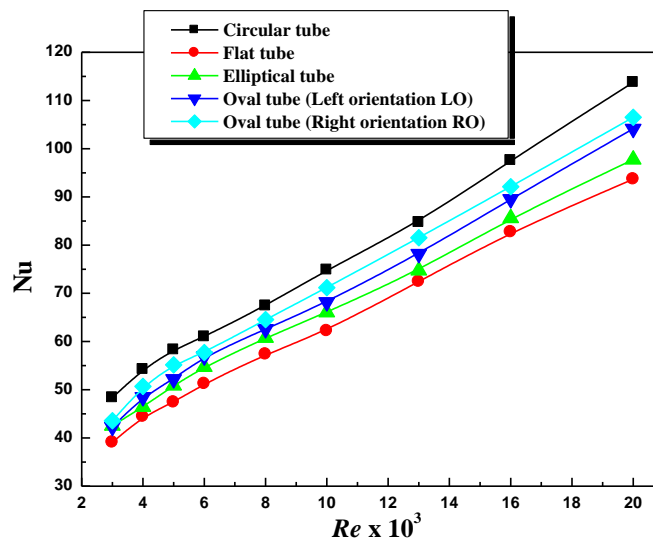


Figure 6. Variation of the Nusselt number vs. Reynolds number.

Table 3. Prediction of the Nusselt number.

$Nu = C \times Re^n$ , for $3000 \leq Re \leq 20000$					
	Circular	Flat	Elliptic	Oval LO	Oval RO
$C$	1.4568	1.0242	1.2959	1.1021	1.1884
$n$	0.4326	0.4514	0.4312	0.4532	0.4486
$R^2$	0.9767	0.9881	0.9875	0.9866	0.9882

**Friction Factor**

The distribution of the friction factor vs. Reynolds number is illustrated in Figure 7. This figure shows that the friction factor decreases according to the raise of Reynolds numbers. The maximum values of friction factor are obtained with

the circular tube, followed by the flat tube, oval tube in the right orientation (RO), oval tube in the left orientation (LO), and then the elliptical tube. These results confirmed the conclusions reported by Tahseen et al. [11], where the circular, oval and elliptical tubes ensure practically the same values of heat transfer coefficient. Still, the oval and elliptical tubes create a modest pressure drop compared with the circular tube. Comparing with the flat tube, circular, oval RO, oval LO, and elliptical tubes create a percentage of friction factor of about 10% (higher), 0% (identical), 8% (inferior), and 2% (inferior), respectively. By using the Excel Software and to predict the friction factor, Table 4 summarizes the empirical correlations of each configuration. Where  $R^2$  is the coefficient of determination of correlation.

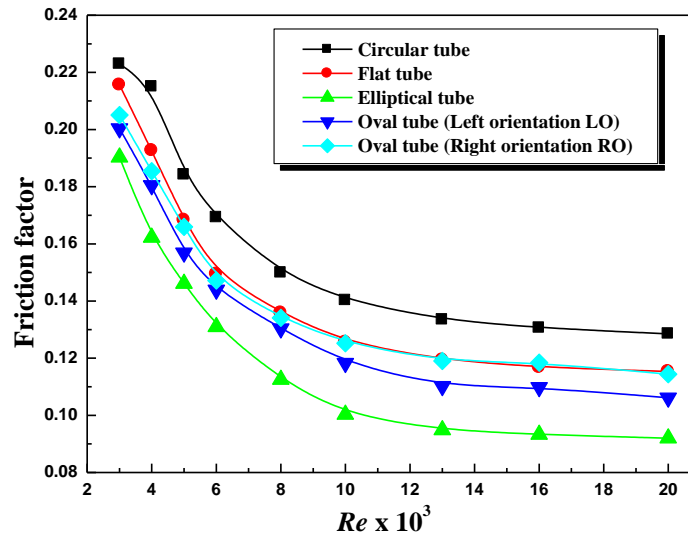


Figure 7. Variation of the friction factor vs. Reynolds number.

Table 4. Prediction of the friction factor.

$f = C \times Re^n$ , for $3000 \leq Re \leq 20000$					
	Circular	Flat	Elliptic	Oval LO	Oval RO
$C$	2.8319	3.1659	4.496	3.1102	2.4872
$n$	- 0.32	- 0.343	- 0.403	- 0.349	- 0.318
$R^2$	0.9409	0.9342	0.9464	0.9546	0.9386

## CONCLUSION

A numerical study was presented in this paper by using the computer code Ansys Fluent. The heat transfer behavior and fluid flow were tested for a range of Reynolds numbers varied from 3000 to 20000. Several configurations of the tube shape and their influences on airflow in a fin and tube heat exchanger have been studied. The results show that the circular-shaped tube ensures the best heat transfer rate compared to other cases. Nevertheless, the elliptical tube yields the lowest pressure losses compared to the other configurations. Where, compared with the flat tube, the circular, oval RO, oval LO, and elliptical tubes ensure a percentage of heat transfer coefficient of about 18, 12, 10, and 4%, respectively. On the other hand, and in the same conditions, circular, oval RO, oval LO, and elliptical tubes create a percentage of friction factor of about 10% (higher), 0% (identical), 8% (lower) and 2% (lower), respectively. Subsequently, reliable correlations have been proposed to predict the Nusselt number and the friction factor.

## NOMENCLATURE

- $C_p$  specific heat [J/kg K]
- $D_h$  hydraulic diameter [m]
- $E_t$  Width of flat tube [m]
- $f$  friction factor [-]
- $h$  heat transfer coefficient [W/m<sup>2</sup> K]
- $G_k$  Turbulent kinetic energy production

$k$  thermal conductivity [W/m<sup>2</sup> K]  
 $Nu$  Nusselt number [ $h D_h / k$ ]  
 $m_f$  mass flow rate [kg/s]  
 $\Delta P$  pressure drop [Pa]  
 $Q$  heat transfer rate [W]  
 $U_m$  mean velocity at the minimum flow cross-sectional [m/s]  
 $Re$  Reynolds number [ $\rho U_m D_h / \mu$ ]  
 $T$  temperature [K]  
 $u$  Mean velocity at the channel (m/s)  
 $u_i$  Axial velocity (m/s)  
 $u_j$  Vertical velocity (m/s)

*Greek letters*

$\mu$  dynamic viscosity [kg/m s]  
 $\rho$  density [kg/m<sup>3</sup>]

*Subscript*

$in$  inlet  
 $m$  mean  
 $out$  outlet  
 $w$  wall

*Abbreviation*

*FTHEs* fin and tubes heat exchanger

## REFERENCES

- [1] B. E. Launder and T. H. Massey, "The numerical prediction of viscous flow and heat transfer in tube banks," *ASME Journal of Heat Transfer*, vol. 100, pp. 565-571, 1978.
- [2] A. Zukauskas, "Heat transfer from tubes in cross flow," in *Advances in Heat Transfer*. vol. 8, ed, 1972, pp. 93-160.
- [3] M. Fujii and T. Fujii, "A numerical analysis of laminar flow and heat transfer of air in an in-line tube bank," *Numerical Heat Transfer*, vol. 7, pp. 89-102, 1984.
- [4] E. M. Sparrow and S. Kang, "Longitudinally-finned cross-flow tube banks and their heat transfer and pressure drop characteristics," *International journal of heat and mass transfer*, vol. 28, pp. 339-350, 1985.
- [5] J. Baughn, M. Elderkin, and A. McKillop, "Heat transfer from a single cylinder, cylinders in tandem, and cylinders in the entrance region of a tube bank with a uniform heat flux," 1986.
- [6] M. Faghri and N. Rao, "Numerical computation of flow and heat transfer in finned and unfinned tube banks," *International journal of heat and mass transfer*, vol. 30, pp. 363-372, 1987.
- [7] G. Stanescu, A. Fowler, and A. Bejan, "The optimal spacing of cylinders in free-stream cross-flow forced convection," *International journal of heat and mass transfer*, vol. 39, pp. 311-317, 1996.
- [8] Z. Guo, D. Li, and B. Wang, "A novel concept for convective heat transfer enhancement," *International journal of heat and mass transfer*, vol. 41, pp. 2221-2225, 1998.
- [9] B. Anoop, C. Balaji, and K. Velusamy, "A characteristic correlation for heat transfer over serrated finned tubes," *Annals of Nuclear Energy*, vol. 85, pp. 1052-1065, 2015.
- [10] S. Beale and D. Spalding, "A numerical study of unsteady fluid flow in in-line and staggered tube banks," *Journal of Fluids and Structures*, vol. 13, pp. 723-754, 1999.
- [11] T. A. Tahseen, M. Ishak, and M. Rahman, "An overview on thermal and fluid flow characteristics in a plain plate finned and un-finned tube banks heat exchanger," *Renewable and Sustainable Energy Reviews*, vol. 43, pp. 363-380, 2015.
- [12] N. Benarji, C. Balaji, and S. Venkateshan, "Unsteady fluid flow and heat transfer over a bank of flat tubes," *Heat and mass transfer*, vol. 44, p. 445, 2008.
- [13] T. Fullerton and N. Anand, "Periodically fully-developed flow and heat transfer over flat and oval tubes using a control volume finite-element method," *Numerical Heat Transfer, Part A: Applications*, vol. 57, pp. 642-665, 2010.
- [14] M. Ishak, T. A. Tahseen, and M. M. Rahman, "Experimental investigation on heat transfer and pressure drop characteristics of air flow over a staggered flat tube bank in crossflow," *International Journal of Automotive and Mechanical Engineering*, vol. 7, p. 900, 2013.
- [15] T. A. Tahseen, M. Ishak, and M. Rahman, "An Experimental Study Air Flow And Heat Transfer Of Air Over In-Line Flat Tubebank," in *International Conference on Mechanical Engineering Research (ICMER2013)*, 2013, p. 3.
- [16] T. A. Tahseen, M. Ishak, and M. Rahman, "An experimental study of heat transfer and friction factor characteristics of finned flat tube banks with in-line tubes configurations," in *Applied Mechanics and Materials*, 2014, pp. 197-203.

- [17] H. M. Bahaidarah, N. Anand, and H. Chen, "A numerical study of fluid flow and heat transfer over a bank of flat tubes," *Numerical Heat Transfer, Part A: Applications*, vol. 48, pp. 359-385, 2005.
- [18] S. S. Yogesh, A. S. Selvaraj, D. K. Ravi, and T. K. R. Rajagopal, "Heat transfer and pressure drop characteristics of inclined elliptical fin tube heat exchanger of varying ellipticity ratio using CFD code," *International journal of heat and mass transfer*, vol. 119, pp. 26-39, 2018.
- [19] J. Li, C. Dang, and E. Hihara, "Heat transfer enhancement in a parallel, finless heat exchanger using a longitudinal vortex generator, Part B: Experimental investigation on the performance of finless and fin-tube heat exchangers," *International journal of heat and mass transfer*, vol. 128, pp. 66-75, 2019.
- [20] J. Li, C. Dang, and E. Hihara, "Heat transfer enhancement in a parallel, finless heat exchanger using a longitudinal vortex generator, Part A: Numerical investigation," *International journal of heat and mass transfer*, vol. 128, pp. 87-97, 2019.
- [21] M. Ma'arof, G. T. Chala, H. Husain, and M. S. Mohamed, "Influence of fins designs, geometries and conditions on the performance of a plate-fin heat exchanger-experimental perspective," *Journal of Mechanical Engineering and Sciences*, vol. 13, pp. 4368-4379, 2019.
- [22] D. Sahel, H. Ameer, and Y. Kamla, "A numerical study of fluid flow and heat transfer over a fin and flat tube heat exchangers with complex vortex generators," *The European Physical Journal Applied Physics*, vol. 78, p. 34805, 2017.
- [23] H. Han, Y.-L. He, Y.-S. Li, Y. Wang, and M. Wu, "A numerical study on compact enhanced fin-and-tube heat exchangers with oval and circular tube configurations," *International journal of heat and mass transfer*, vol. 65, pp. 686-695, 2013.
- [24] A. M. Lavasani, H. Bayat, and T. Maarefdoost, "Experimental study of convective heat transfer from in-line cam shaped tube bank in crossflow," *Applied thermal engineering*, vol. 65, pp. 85-93, 2014.
- [25] T. A. Tahseen, M. Ishak, and M. Rahman, "Performance predictions of laminar heat transfer and pressure drop in an in-line flat tube bundle using an adaptive neuro-fuzzy inference system (ANFIS) model," *International Communications in Heat and Mass Transfer*, vol. 50, pp. 85-97, 2014.
- [26] Y.-H. Zhang, L.-B. Wang, F. Ke, Y. Su, and S. Gao, "The effects of span position of winglet vortex generator on local heat/mass transfer over a three-row flat tube bank fin," *Heat and mass transfer*, vol. 40, pp. 881-891, 2004.
- [27] M. Mellal, R. Benzeguir, D. Sahel, and H. Ameer, "Hydro-thermal shell-side performance evaluation of a shell and tube heat exchanger under different baffle arrangement and orientation," *International Journal of Thermal Sciences*, vol. 121, pp. 138-149, 2017.
- [28] D. Sahel, H. Ameer, R. Benzeguir, and Y. Kamla, "Enhancement of heat transfer in a rectangular channel with perforated baffles," *Applied thermal engineering*, vol. 101, pp. 156-164, 2016.
- [29] D. Sahel and R. Benzeguir, "Thermal characteristic in solar air heater fitted with plate baffles and heating corrugated surface," *Energy Procedia*, vol. 139, pp. 307-314, 2017.
- [30] S. Eiamsa-ard and P. Promvonge, "Numerical study on heat transfer of turbulent channel flow over periodic grooves," *International Communications in Heat and Mass Transfer*, vol. 35, pp. 844-852, 2008.
- [31] H. Ameer and D. Sahel, "Effect of some parameters on the thermohydraulic characteristics of a channel heat exchanger with corrugated walls," *Journal of Mechanical and Energy Engineering*, vol. 3, 2019.
- [32] K. Boukhadia, H. Ameer, D. Sahel, and M. Bozit, "Effect of the perforation design on the fluid flow and heat transfer characteristics of a plate fin heat exchanger," *International Journal of Thermal Sciences*, vol. 126, pp. 172-180, 2018.
- [33] H. Ameer, "Effect of the baffle inclination on the flow and thermal fields in channel heat exchangers," *Results in Engineering*, vol. 3, p. 100021, 2019.
- [34] H. Ameer and Y. Menni, "Laminar cooling of shear thinning fluids in horizontal and baffled tubes: Effect of perforation in baffles," *Thermal Science and Engineering Progress*, vol. 14, p. 100430, 2019.
- [35] H. Ameer, "Effect of Corrugated Baffles on the Flow and Thermal Fields in a Channel Heat Exchanger," *Journal of Applied and Computational Mechanics*, vol. 6, pp. 209-218, 2020.
- [36] D. Sahel, H. Ameer, and W. Boudaoud, "A new correlation for predicting the hydrothermal characteristics over flat tube banks," *Journal of Mechanical and Energy Engineering*, vol. 3, pp. 273-280, 2019.
- [37] H. Ameer, D. Sahel, and Y. Menni, "Enhancement of the cooling of shear-thinning fluids in channel heat exchangers by using the V-baffling technique," *Thermal Science and Engineering Progress*, p. 100534, 2020.
- [38] T. Kim, "Effect of longitudinal pitch on convective heat transfer in crossflow over in-line tube banks," *Annals of Nuclear Energy*, vol. 57, pp. 209-215, 2013.